Escherichia Coli Swim back Towards Stiffer Polyetheylene glycol Coatings, increasing Contact in Flow

Molly K. Shave,[1] Zhou Xu,[2] Vishnu Raman,[3] Surachate Kalasin,[1] Mark T. Tuominen,[2] Neil S. Forbes,[3] Maria M. Santore[*1]

1. Department of Polymer Science and Engineering, University of Massachusetts, Amherst, MA 01003
2. Department of Physics, University of Massachusetts, Amherst, MA 01003
3. Department of Chemical Engineering, University of Massachusetts, Amherst, MA 01003

corresponding author: Maria M. Santore
Department of Polymer Science and Engineering
University of Massachusetts at Amherst
120 Governors Drive
Amherst, MA 01003
santore@mail.pse.umass.edu

Abstract

Bacterial swimming in flow near surfaces is critical to the spread of infection and device colonization. Understanding how material properties affect flagella- and motility- dependent bacteria-surface interactions is a first step in designing new medical devices that mitigate the risk of infection. We report that, on biomaterial coatings such as polyethylene glycol (PEG) hydrogels and end-tethered layers that prevent adhesive bacteria accumulation, the coating mechanics and hydration control the near-surface travel and dynamic surface contact of *E. coli* cells in gentle shear flow (order 10 s^{-1}). Along relatively stiff (order 1 MPa) PEG hydrogels or end-tethered layers of PEG chains of similar polymer correlation length, run and tumble *E. coli* travel nanometrically close to the coating's surface in the flow direction in distinguishable runs or "engagements" that persist for several seconds, after which cells leave the interface. The duration of these engagements was greater along stiff hydrogels and end-tethered layers compared with softer more hydrated hydrogels. Swimming cells that left stiff hydrogels or end tethered layers proceeded out to distances of a few microns and then returned to engage the surface again and again, while cells engaging the soft hydrogel tended not to return after leaving. As a result of differences in the duration of engagements and tendency to return to stiff hydrogel and end-tethered layers, swimming *E. coli* experienced three times the integrated dynamic surface contact with stiff coatings compared with softer hydrogels. The striking similarity of swimming behavior near 16 nm thick end-tethered layers and 100 μm thick stiff hydrogels argues that only the outermost several nanometers of a highly hydrated coating influence cell travel. The range of material stiffnesses, cell-surface distance during travel, and timescales of travel compared with run and tumble timescales suggests the influence of the coating derives from its interactions with flagella and its potential to alter flagellar bundling. Given that restriction of flagellar rotation is known to trigger increased virulence, bacteria influenced by surfaces in one region may become predisposed to form a biofilm downstream.

Keywords: hydrodynamics, active matter, biofilm formation, bacterial adhesion, surface interactions, mechanics, motility, swimming, microswimmers, force, dynamic adhesion, trajectory, residence time, flow, shear stress, attachment, biocompatible

Introduction

The role of cell adhesion in biofilm formation[1] has driven development of materials that limit accumulation of bacteria. Hydrophilic water-swollen surfaces, from sub-millimeter hydrogel coatings to molecular layers of tethered polymers, have come to prominence as they can nearly eliminate protein and bacterial capture *in vitro*.[2-4] Even so, device-related infections persist,[5-9] prompting a closer examination of bacteria-surface interactions with minimally adhesive coatings. Coatings that reduce but do not eliminate cell capture are associated with significant numbers of infections, suggesting mechanisms that are not well-anticipated by classical assays, based on cells retained after rinsing.[10]

Understanding the interfacial environment is important because it supports bacteria phenotypes of increased virulence relative to planktonic cells,[1] thereby facilitating biofilm formation.[1, 11, 12] Near surfaces, for instance, restricted flagellar motion can trigger upregulation of virulence factors.[13, 14] It may therefore be the case that weakly adhesive materials, attracting but not arresting cells, could similarly trigger a cell-level response, even as the cells progress along a surface. Since motile bacteria are known to swim along surfaces for extended periods,[15-18] they may be influenced by dynamic adhesive contact. Indeed, mechanics are well known to influence weak reversible adhesion[19] through dissipation in the near-interface bulk material. This suggests that the stiffness of a biomaterial coating should be considered *especially* in the case of weak reversible cell adhesion. This work therefore examines the impact of coating stiffness on bacterial interactions at surfaces where, despite evidence for attractive interactions, flowing swimming cells are not arrested.

Cell-surface interactions can be physico-chemical or hydrodynamic. Relevant to the latter, *E. coli* express multiple flagellae and swim via a "pushing" mechanism where a rotating flagellar bundle pushes the cell forward and fluid to the back. This is balanced by an inward draw of fluid towards the cell's equator, producing a force dipole having a range on the order of the cell itself.[20] Pusher type swimming attracts the sides of cells towards surfaces[20] and stabilizes near-surface travel. *E. coli* have been reported to swim 2-5 μm,[20] 0.2-0.3μm,[21] 10-60 nm,[22] or 30-40 nm[18] from rigid walls in quiescent conditions. In wild-type *E. coli* and also in the cells of this study, temporary motor reversal causes flagellae to unbundle and cells to tumble. Subsequent motor rotation and rebundling re-engages swimming. This "run and tumble" motion contrasts genetically engineered "Smooth swimming" *E. coli* employed in other studies.

In quiescent conditions, both run-and-tumble and smooth swimming *E. coli* swim in protracted runs or "engagements" along surfaces.[15-18] Elevated concentrations of pusher swimmers, relative to the bulk solution concentration, have been observed near solid surfaces,[20, 23] consistent with models for fluxes of swimming cells.[20] Smooth swimming *E. coli* follow circular clockwise trajectories (when viewed from above the surface or behind the cell) near rigid walls.[15, 22] Opposite circling at air-water interfaces[24] has been attributed to interfacial slip.[25] Thus, hydrodynamic slip at a wall has been suggested as a mechanism for surface influence on bacterial swimming.[25, 26]

Cell orientation due to shear can produce distinctive swimming behaviors. In Poiselle flow swimming cells can orient and become trapped in regions of high shear,[27] an effect not requiring proximity to a wall. Near surfaces and with low fluid velocity, cells can be oriented and visibly

swim against the flow (rheotaxis).[28, 29] Rheotaxis and shear trapping are often dominated by net flow outside particular ranges of system parameters.

Important questions remain regarding the combined influence of flow and surface properties on bacterial swimming and surface interactions. For instance, it was recently discovered that surface encounters can alter the rebundling times of run-tumble *E. coli*, altering swimming itself.[30] Of particular interest is how surfaces can alter the behavior of cells at the level of populations, for instance the duration and distance of cell contact with minimally adhesive surfaces in flow, the distributions of these residence times, and the trajectories themselves. The current study therefore probes the impact of surface mechanics on dynamic cell residence times and quantifies how interactions with surfaces of different stiffness and water content affect features of the swimming trajectories at the levels of distributions.

Focusing on coatings of polyethylene glycol (PEG) hydrogels and end-tethered layers (brushes) which do not retain bacteria in flow, we address the influence of coating stiffness and water content on the near-surface motion of gently flowing swimming *E. coli*. Run and tumble swimmers are compared to a non-motile strain that lacks flagellar motors. *E. coli* have been reported to adhere somewhat on the PEG hydrogel soft this study after settling in gravity for 24 hours.[31] However, swimming cells are not captured in the current study, which employs a flow chamber oriented so that gravity does not pull cell towards test surfaces. The current study also employs a wide gap flow chamber so that cells interact with a single material surface. Tracking the time-dependent positions of near-surface cells reveals trajectories and enables the cell-wall distance to be approximated from existing hydrodynamic models. For coatings of different

stiffness, thickness, and water content, we report differences in velocity distributions of *E. coli* cells in surface-associated runs termed "engagements." These engagements, in the current study in flow, are analogous to near surface trajectories reported for quiescent conditions.[15, 16] We report a discovery that the coating's mechanical properties /water content influence swimming sufficiently to impact cell escape and return to the surface. As a result, stiffer hydrogels have substantially more extensive dynamic contact with swimming cells. These findings provide new perspective on the design of biomaterials that reduce the risk of infection.

Background

This study employed polyethylene glycol (PEG) coatings; either swollen crosslinked hydrogel films or molecularly-thin end-tethered layers of PEG chains, represented in Figure 1. These materials were previously characterized[32] and their properties are summarized in Table I. The thickness difference between the ~100 μm-thick swollen hydrogels and tethered linear chains layers addresses any impact of the underlying rigid microscope slide substrate. PEG coatings, if prepared with sufficient uniformity, density, and appropriate surface attachment, are among the least adhesive coatings for biomaterial applications.[2-4] As a large degree of hydration is required for reduced bioadhesion, the hydrogel films employed here comprised either ~50 or ~90% water by volume. However, the electronegativity of PEG's ether oxygens are known to attract to cationic groups on proteins and cell surfaces.[33, 34] PEG forms hydrogen bonds as an acceptor,[35] and sufficiently recognized by the body to enable antibody formation.[36, 37] These physico-chemical interactions may also be at play during transient bacterial interactions.

Table I. Properties of PEG Hydrogels and Tethered PEG Layers[32, 33]

Sample	Water Content	G' (hydrogels) G (tethered layer), kPa	Correlation Length, ξ	Coating thickness
Tethered Layer	94 ±2%	450	2.9 ±0.1 nm	16 ±1.5 nm
Stiff Hydrogel	54 ±1%	1300	1.0 ±0.1 nm	100 μm
Soft Hydrogel	91 ±2%	9.5	2.7 ±0.1 nm	100 μm

In the current hydrogel coatings, hydrated PEG chains between crosslinks are swollen or "perturbed" random coils. The through-space distance between crosslinks, estimated previously from swelling data,[31, 32] is reported in Table I and represents a correlation length.[38] Layers of tethered PEG chains are formed by the effectively irreversible adsorption of PEG-containing copolymers from aqueous solution to treated slides.[39, 40] Careful molecular design ensures sufficiently dense PEG grafting to shield the substrate and also avoids trapping or entanglements

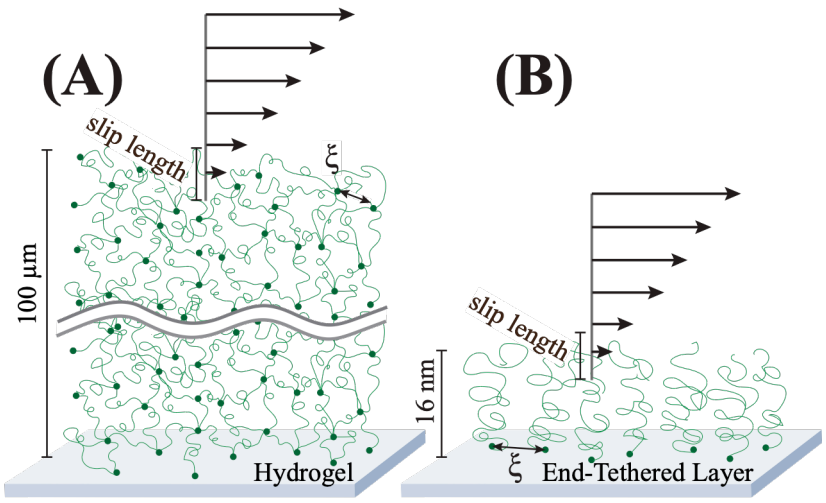

Figure 1. Schematic of (A) hydrogel coating and (B) layer of end tethered chains, showing that flow penetrates these hydrated coatings only slightly, by the slip length. The correlation length, ξ, is also shown.

that would expose adhesive anchoring functionality.[40, 41] With average distances between grafted chains smaller than the free coil size of the PEG chains, the tethered chains stretch normal to the surface, but can locally be described as self-avoiding walks,[42, 43] similar to the PEG chains between crosslinks in the hydrogel. In the tethered layer, the average distance between tether points, known from the PEG molecular weight and the amount immobilized on the surface,[39, 44] is also a correlation length[42] In this study the correlation length of the tethered layer is chosen in the same range as that for the hydrogels. Thus, despite the four order of magnitude difference in coating thickness, the hydrogel films and the molecular PEG layers fall in a similar physical regime.

In shear flow past end-tethered layers and swollen hydrogels, the hydrodynamic field is thought to penetrate only about a correlation length into the coating. Thus the correlation length provides a measure of the hydrodynamic screening length.[45-47] Thus, despite the large water content within the coatings, flow occurs only in the outermost few nanometers of the coating. This flow

penetration depth, on the order of the correlation length represents a slip length in Figure 1. It has been suggested that even nanometric differences in slip lengths should influence the swimming of nearby bacteria in quiescent conditions.[25] In the current work, variations in the crosslink density affect coating stiffness and the degree of swelling or water content, preventing decoupling of these properties.[38] In fact, the compression of hydrated coatings is essentially an osmotic process because compressing a hydrogel or tethered layer requires squeezing fluid out.[43, 44] This fact enables the brush compressibility, requiring deformations of just 1-4 nm, not easily achievable in characterization experiments, to be calculated as reported previously.[32] Meanwhile the moduli of the hydrogels, previously measured[31, 32] are summarized alongside in Table I.

This study employed an *E. coli* strain having flagella expression regulated by an arabinose switch, and a non-motile control *E. coli* strain expressing flagella but lacking operational motors.

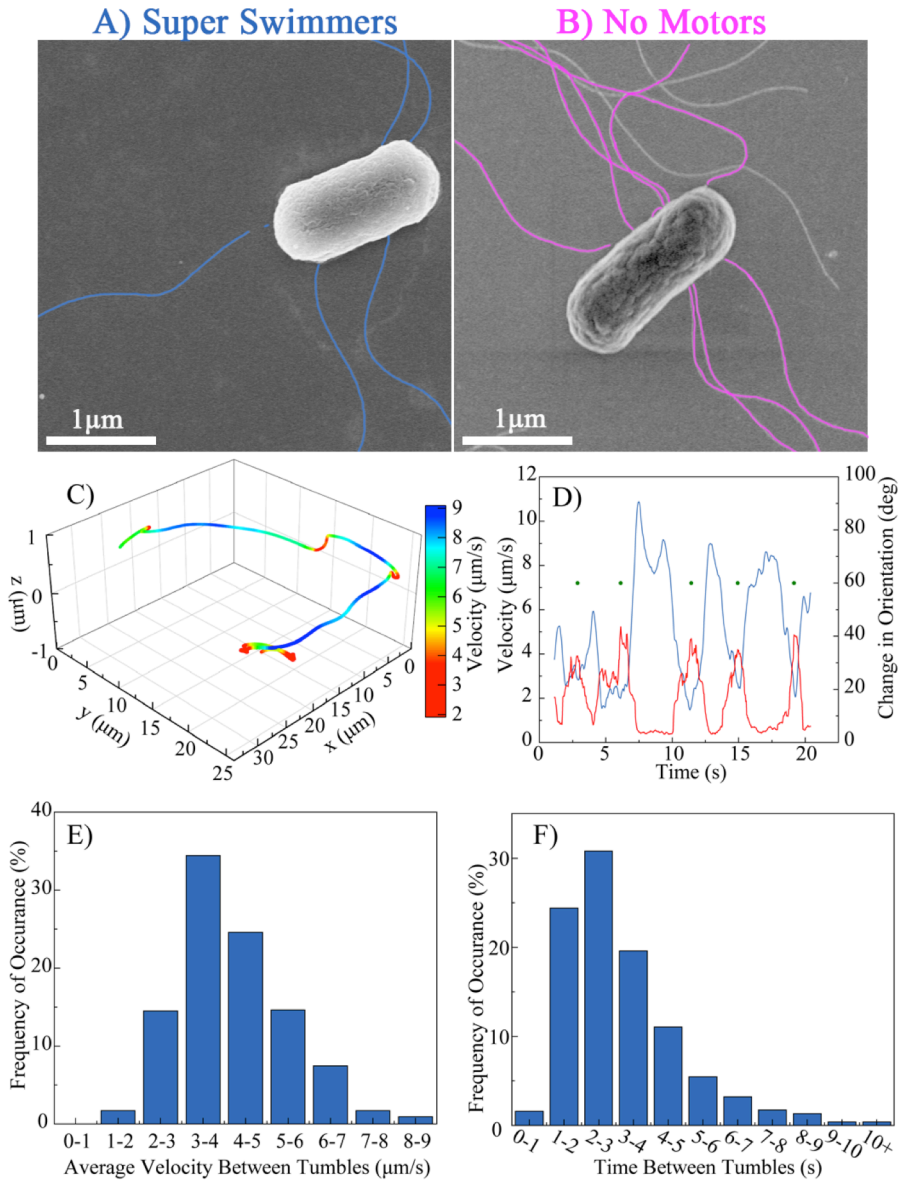

Figure 2. Electron micrographs of typical (A) motile "swimmers" and (B) no-motor non-motile *E. Coli* cells, with flagella highlighted. (C) Typical trajectory of motile "swimmer" cell and (D) velocity and rotation along a trajectory consistent with run/tumble behavior. (E) Distribution of average run velocities between tumbles for swimmers and (F) distribution duration of run times between tumbles for swimmers.

The electron micrographs of Figure 2A and B illustrate typical cell sizes near 0.75 x 2 μm, and confirm expression of flagella in both strains. Motility assays in the Supporting Information confirm that the swimmers were highly motile and the no-motor strain was entirely non-motile. The run and tumble character of the swimmers was confirmed by tracking, in Figure 2C. Per the example in Figure 2D, analysis of the trajectory via the approach of Qu *et al*.,[30] identified periods of fast swimming and periods of slow velocity where the latter exhibited directional changes. For 754 cells, velocities during the run phases are summarized, along with times between swimming runs in Figures 2-E and F, respectively. In accord with prior descriptions of run-and-tumble movements, the swimming velocities were consistent for multiple run phases of each cell, but the swimming speed itself was cell-dependent, with some cells swimming faster than others,[30] mostly in the range 3-6 μm/s.

Results

Features of near-wall trajectories of flowing cells. Bacterial suspensions (~1 x 10^8 cells/ml) were flowed through a 800 μm-deep channel at a volumetric flow rate of 45 ml/hr corresponding to a wall shear rate of 15 s^{-1}. Focusing the microscope at the free surface of the PEG coating (with a field of 178 x 260 μm, the latter in the flow direction), large numbers of near-surface cells were video recorded over several minutes. Cells did not arrest but traveled with the fluid, slowing when they encountered the PEG coating. A vertical chamber orientation in Figure 3A avoided the issue of gravity pulling cells towards or away from the interface. The large channel depth enabled study of cell interactions with a single wall. In the 40 microns nearest the coating, the velocity is well described (< 5% error) by the product of the wall shear rate and the distance from the coating. Streamlines further from the surface correspond to higher velocities.

Typical trajectories, for swimmers and non-motile controls in Figure 3B illustrate how the flow and encounters with the coating influenced cell travel near a coating's surface. Here data points have a time spacing of 0.2 s, and colors represent instantaneous velocities. Thus closer data points indicate slower travel. Variations in cell velocity for theses trajectories are summarized in Figures 3C - F, revealing important features of cell travel along the PEG coatings: hopping between streamlines away from the surface and, near to the surface, slower smoother travel, which we denote as "engagements". In Figure 3, engaged cells traveling near the surface occasionally escape from the interface and reach faster streamlines, later sometimes returning to the interface for additional surface-engaged travel. Specific metrics, developed below, provide a statistical quantitative measure of the influence of coating interactions on the motion of swimmers and non-motile control cells. The velocities are further interpreted by applying hydrodynamic models.

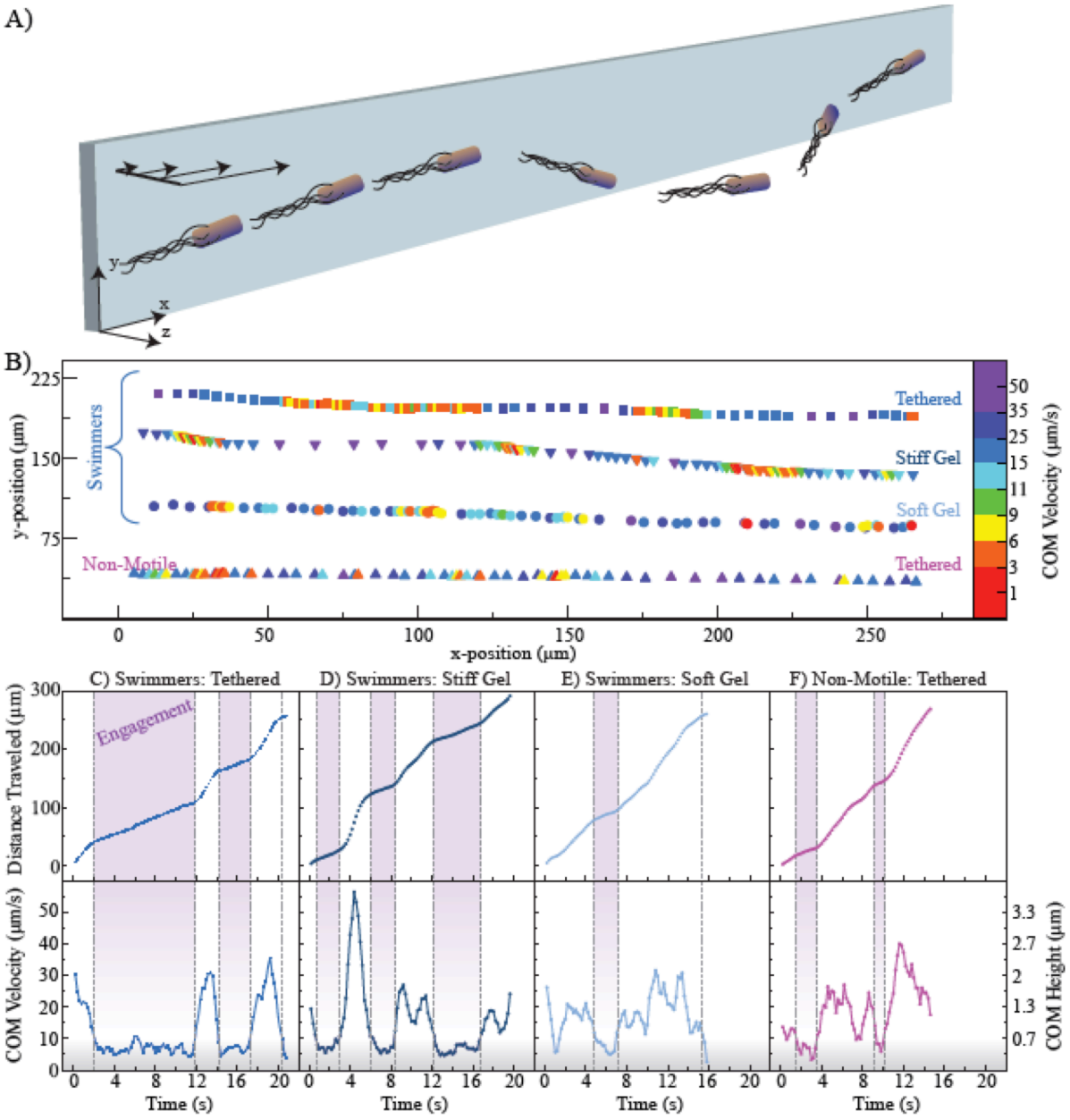

Figure 3. (A) Schematic of flow chamber and orientation showing a swimming cell engaged, coming off, and returning to the surface in flow. Cell orientation is not intended to be meaningful or known. (B) Trajectories for three example swimmer cells flowing over three different PEG surfaces and an example non-motile cell flowing over an end-tethered PEG surface. The wall shear rate is 15 s^{-1}. x is the flow direction and y is the in-plane perpendicular direction. z is normal to the surface. Points are 0.2 s apart. Trajectories are shifted in the y-direction to facilitate viewing. (C)-(F) report the total distance traveled starting at the time the cell appeared in the field of view, along with the instantaneous COM (center of mass) velocities (C) for a swimmer by an end-tethered layer (D) for a swimmer by a stiff gel (E) for a swimmer by a soft gel and (E) for a non-motile cell by an end-tethered layer. Vertical shaded regions highlight periods of slow velocity caused by engagement with the PEG coating. The slow velocity range where these engagements most likely occur is highlighted across the bottom of the lower panels.

Far field hydrodynamics. Far from the wall, objects travel at a velocity corresponding to the streamline on which they reside. The streamline velocity is the wall shear rate time the distance from the wall. In the Supporting Information, the treatment of Goldman *et al*.[48] approximates when this limit breaks down, with error increasing to 10% as a spherical particle's surface approaches the wall to within 20% of its diameter, here a few hundred nanometers. As a cell is carried downstream in the flow, its instantaneous velocity reveals its distance to the wall as long as it is further than a few hundred nanometers. The right axis of Figures 3F therefore employs the measured the velocities on the left axis to calculate the approximate center of mass heights from the wall shown on the right axis, for the non-motile bacteria, for $\gamma = 15\ s^{-1}$ in this far field limit. The estimates on the right axis of Figure 3F do not go down beyond about a half of a micron, and should also roughly apply for swimming cells far from the wall since streamline velocities of 15-40 μm/s substantially exceed speeds measured for the bacterial run phase (3-6 μm/s) in Figure 2E. That is, for instance, when swimmers are observed to travel above 15 μm/s they do so because they are transported by the flow on the corresponding streamline.

Closer to the surface. The observed periods of slow travel, termed "engagements" in Figure 3C-F prompt estimates for the distance between *E. coli* bodies and the surface. An analysis in the Supporting Information based on Goldman *et al.*,[48] treats the cell bodies as spheres as a first estimate while accounting for hydrodynamic interactions with the wall, an approach which remains useful even recently.[18, 22, 49] In the case of a 2 μm sphere, for instance, travel at 10 μm/s corresponds to a fluid gap at the wall of less than 35 nm while a 9 μm/s velocity corresponds to a gap of 22 nm. A 2 μm sphere traveling at 6 μm/s has an approximate gap of 1 nm with a rigid wall and would be in effective contact with the PEG coatings in this study. For the velocities of

the engagements of the cells in Figure 3, in the range below 9-10 μm/s, these approximate nanometric separations are smaller than the cell-wall gaps reported for swimming cells in quiescent conditions, from microns down to 30 nm.[18, 20-22]

The potentially small gaps and opportunity for dynamic physico-chemical interactions of slow-traveling *E. coli* with the coatings focused our attention on cells experiencing sustained stretches of slow near-surface motion or engagements. Avoiding reliance on overly simplistic treatments to quantify the cell-coating gap, we note that the measurements of velocity could be used in future sophisticated models for near-surface bacteria swimming in flow. The analysis below, however, requires no assumptions about the cell separation from the coating.

Defining Cell Engagement. Quantifying the impact of the coating on cell travel requires dynamically surface-engaged cells to be discriminated from the thousands of cells passing through the field of view in each run. To be counted as dynamically "engaged" and further analyzed, cells were required to travel below a velocity threshold of 9.3 μm/s for a travel distance of at least 5 μm (about twice the cell body length and corresponding to an engagement time of least 0.6 s). The Supporting Information demonstrates that the exact choice of threshold, for instance 9.3 versus 11.3 μm/s, had a minimal impact on the distributions of various metrics and did not affect the conclusions of this study. By excluding cells that never reached the surface or collided only briefly, the analysis focuses on cells with stronger hydrodynamic and possible physico-chemical interactions with the PEG-coated wall.

Influence of Coating on Individual Engagements. Figure 4 summarizes the distributions of engagement velocities and engagement durations (interfacial residence times) for swimming and

non-motile cells on the three coatings, for 20-35 cells /run and 3 surfaces/bacterial preparations for each cell-surface combination. In Figures 4A and B, there is a marked and statistically significant difference (exceeding 99% certainty, summarized in the Supporting Information) in engagement velocity between swimmers and non-motile cells with the non-motile cells moving more rapidly along streamlines than the swimmers. This could be explained by two effects: First, while swimmers were not observed to translate upstream, the slower observed velocities of the swimmers might be attributed to their orientation by shear to swim against the flow with a slower net velocity in the flow direction. A second and likely possibility is that, relative to non-motile cells, swimmers reside slightly closer to the coating surfaces, sampling slower moving streamlines. Evidence for the closer proximity of the swimmers to the coatings is seen in the small but statistically significant material-dependent velocities of the swimmers, absent from the velocity distribution of non-motile cells. In particular, near layers of tethered chains and stiff hydrogel surfaces, very slow moving populations introduce slow tails into the velocity distributions.

Also summarized in Figure 4 are distributions of durations of engagements, which can be treated

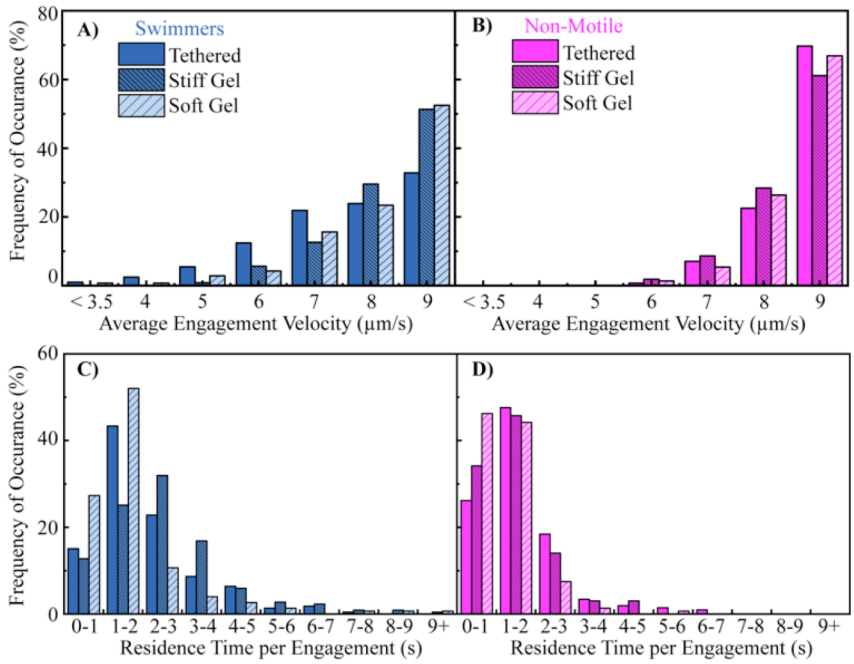

Figure 4. Distributions of average engagement velocities for (A) swimming cells in blues and (B) non-motile cells in pinks on different PEG coatings and distributions residence times of engagements for (C) swimming cells in blues and (D) non-motile cells in pinks.

as dynamic surface residence times. Figure 4C reveals long time tails in the residence time distributions of swimmers near tethered chains or stiff hydrogels, and a less significant tail in the distribution for swimmers near soft hydrogels. For instance, 42% of swimmer engagements on the tethered PEG layer exceed 2 seconds and 62% of swimmer engagements on the stiff hydrogel exceed 2 seconds. By contrast, only 21% of swimmer engagements on the soft hydrogel exceed 2 seconds. The engagement durations of non-motile control cells are shorter still. Thus larger populations of swimming cells that have long duration engagements stiff PEG compared with soft hydrogels. Further, from the perspective of residence time distributions, the travel of swimmers near the soft hydrogel resembles that of non-motile cells near any of the three surfaces.

It is interesting to ask why cells leave an interface thereby terminating engagements, and if tumbling via flagellar unbundling causes cells to leave the interface. The residence time distributions of near-surface swimmers in Figure 4C are shorter, by about 1-2 s, than the run time distributions of swimmers in quiescent bulk solution in Figure 2F. This suggests that 1) random fluctuations in swimming direction, influenced by the vorticity produce collisions that drive cells off the interface or 2) that swimming along a PEG surface in flow influences flagella bundling and tumbling itself. Previous evidence for the influence of viscous forces on run and tumble swimming[30, 50] supports the existence a mechanism by which different coatings influence the engagement time distributions of Figure 2F. Specifically, viscous forces hinder flagellar rebundling, favoring greater periods of diffusive cell motion.[30]

Material Influence on the Tendency to Engage and Return. The most dramatic impact of the PEG coating on near-surface swimming occurs immediately after a cell escapes an engagement. Figure 5A reveals a great tendency for swimming cells to return, usually after a few seconds, to stiff hydrogel or tethered PEG coatings for additional engagements downstream. There is a far lower return frequency of swimmers to soft hydrogel coatings. The clear impact of the coating on the tendency to return is born out in the non-overlapping error bars (representing standard deviations) for the soft gel versus the other coatings. More specifically, for cells engaging the surface at least once during their travel in the 260 μm-long viewing window, Figure 5 counts the

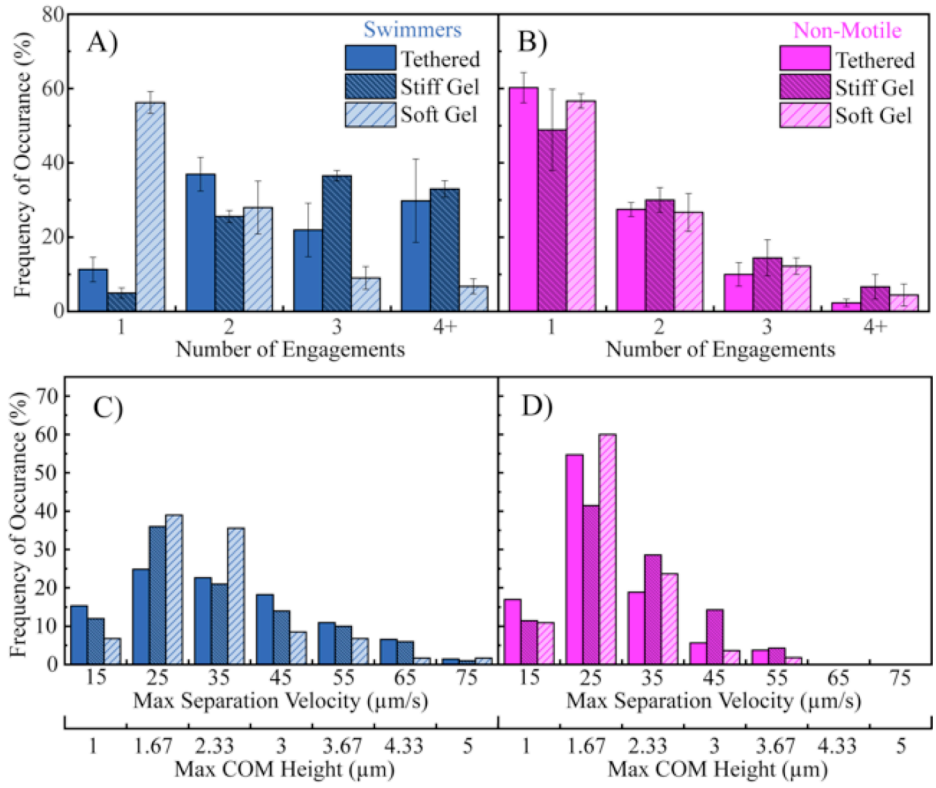

Figure 5. Distributions of numbers of engagements per cell within the field of view for (A) swimmers and (B) non-motile cells. In (A) and (B) error bars represent standard deviations. Distributions of maximum velocities between engagements and the translation of these velocities to furthest center of mass distance (COM) from surface between engagements for (C) swimmers and (D) non-motile cells.

total numbers of engagements per cell. Though these particular engagement numbers depend on the length of the viewing window, one would expect for non-motile (diffusing) cells, that the frequency of multiple engagements decreases with engagement number: Said differently, of diffusing cells experiencing a first engagement, one expects only a fraction will return for a second or third surface engagement within the viewing window, confirmed for the non-motile cells in Figure 5B. By contrast, motile cells near stiff surfaces return repeatedly to a wall coated with a tethered PEG layer or stiff hydrogel. The hallmark tendency of individual swimming cells to return to relatively stiff tethered layers and stiff hydrogels is so great that cells encountering these surfaces only once account for 8 % of the engaging swimming cells, for instance the leftmost dark blue bars in Figure 5A. 92% of swimming cells that engage these surfaces exhibit repeat engagements in a 260 μm-long window (obtained by summing the other 3 dark blue bars in Figure 5A). Near soft hydrogels, swimming cells have a return frequency that is statistically identical to that of the non-motile cells. Figures 5C and D additionally show that swimmers are able to return to stiff hydrogels and brushes from more somewhat distant faster moving streamlines, compared to swimmers returning to soft hydrogels.

The overall impact of the coating on the dynamic contact of swimming cells with coatings is summarized in Figures 6A and B. The combination of longer-lasting and repeat engagements for individual swimming cells on stiff tethered PEG layers and stiff hydrogels produces, for flow past a quarter of a millimeter of a planar surface about three times greater integrated contact time per interactive swimming cell, compared with softer more watery hydrogel layers. Particularly fascinating is the resemblance of swimming cells near these softer surfaces to the behaviors of

no-motor cells and the fact that nanometric tethered layers and 100 μm-thick stiff hydrogels have a qualitatively similar impact on swimmer behavior.

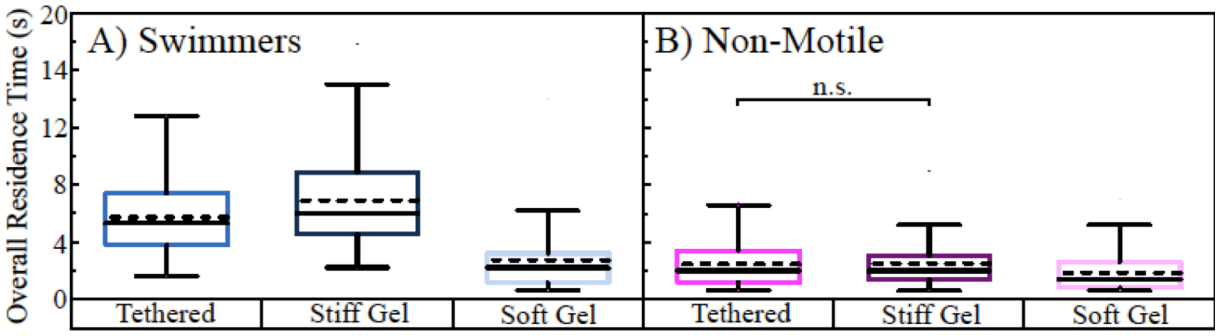

Figure 6. Overall residence times for (A) swimmers and (B) nonmotile cells on different PEG surfaces, summed over all the engagements of each cell within the field of view. In (A), the residence times of the swimmers on the three different PEG surface are all statistically different from each other to at least 99% confidence. In (B) the non-motile cells on the tethered layers and stiff gel surfaces are statistically similar but the non-motile cells on the soft gel compared with either of the other two surfaces is different to at least 99% confidence. Additionally, on the brush and on the stiff gel, the overall residence times of the swimmers was statistically different to more than 99% certainty from the non-motile cells. However, the swimmers and non-motile cells were not statistically different on the soft gel.

Discussion

While hydrodynamic effects (dipolar attractions, shear trapping) can concentrate cells within microns of an interface, the observations reported here indicate a specific influence of the coating material on interfacial bacterial dynamics. The material could play a role either through hydrodynamic, mechanical, or physico-chemical interactions of cells and the PEG coating. These interactions could directly alter cell trajectories but might additionally trigger a "sensing" function, in which flagellar motors rotate differently in response to interfacial forces.

An impact of the material on wall slip is one mechanism by which the coating could influence bacterial travel. With polymer correlation lengths or equivalent slip lengths varying on the scale of nanometers, one estimates that the point of zero shear resides nanometers inside the coating, which acts as a semidilute or concentrated polymer solution. An order of magnitude approximation, for a 5 nm slip length and a wall shear rate of 15 s^{-1} a fluid velocity of 0.075 μm/s is expected in the fluid at the coating surface. Variations in the correlation length would amount to differences in the near-coating fluid velocity of a fraction of this value, seemingly insignificant. However, Hu *et al*.[25] report that a 30 nm slip length is sufficient to eliminate circular swimming. Smaller variations in slip length, of the 2-4 nm range in this study, were not addressed in the literature and would be expected to have less impact.

Mechanisms such as rheotaxis and those involving dynamic contact of cells with the coatings are plausible explanations for the observed slower swimmer velocities compared with no-motor cells. In the case of the rheotaxis, orientation of the cell would enable a component of the swimming velocity against the flow, slowing the cell's progression. Alternately, the coating may

provide viscous resistance to swimmers that are nanometrically close to the surface. For instance the treatment of Goldman *et al*[48] is shown in the Supporting Information, to predict that for a 2 μm sphere traveling at 7 or 8 μm/s, for instance, the sphere's surface lies 4 or 10 nm, respectively from the point of zero shear, which itself is a few nanometers inside the coating. This situation exposes the body of a cell to a nanometric viscoelastic layer that would provide greater resistance to cell translation. Relative to the more concentrated brush and stiff hydrogel surfaces, the soft hydrogel may provide a less viscous or slipperier interface.

Considering the mechanics of a cell swimming against a coating, swimming thrust forces on the order of a picoNewton[51] are opposed by lubrication and steric forces to prevent adhesion. The picoNewton swimming forces, when directed into the coatings, are not expected to deform the PEG brush and stiff hydrogel coatings, even at the nanometer scale, though nanometric deformation of the soft hydrogel might be possible, as calculated in the Supporting Information. Flagella-coating collisions having pN force, however, may provide a greater interactive stress due to smaller contact area (20 nm x order 1 μm), and individual filaments may be able, side-on, to nanometrically penetrate the surface of the soft hydrogel, also in the Supporting Information. Such nanometric penetration of the sides of rotating filaments against a gel may be equivalent to those filaments experiencing a greater effective viscosity compared with the stiffer, more locally flat coatings. The working of a deformable coating by rotating flagellae dissipates energy, potentially influencing cell progression in flow, and the filament dynamics themselves.[50]

To the extent that flagella slide over or slightly penetrate the different coatings, the coatings themselves might affect flagellar bundling. In Figure 5C, between engagements the cell's center

of mass leaves the interface by as much as 4-5 μm, a separation that can easily be bridged by flagella. Flagella that contact the surface after the cell body leaves may affect whether cells are swimming or tumbling after they leave the surface. Viscosity in the range 1-4 cP reduce the rate of flagellar rebundling after a tumble, producing more diffusive rather than swimming behavior.[30] A diffusive character of swimmers near soft hydrogels is seen in Figure 5A in terms of a lack of tendency to return to the interface, and in Figure 4C in terms of swimmer engagement times with soft hydrogels that resemble those of non-motile cells. It is plausible that the soft hydrogel presents resistance to flagellar motion and rebundling as fibers contact and deform the coating surface, an effect similar swimming in a viscous solution that hindering flagellar rebundling. This in turn would increase the diffusive (slow random walk) character of cell motion near soft hydrogels. By contrast, while the PEG brush and stiff hydrogel are classified broadly as soft materials, they are stiff relative to the forces calculated for bacterial flagella may experience a rigid boundary, where the underlying coating thickness is unimportant. Thus, to the extent that the soft hydrogel is able to reduce the efficiency of rebundling after a tumble, or if the soft hydrogel environment directly triggers unbundling of flagella, swimmers would behave more like non motile cells near the soft hydrogel, as reported here.

Finally, the possibility that the motor itself rotates differently in response to force on the flagellae should not be overlooked. It has been established that differences in motor rotation stemming from local viscosity can influence rebundling times, thereby altering trajectories.[30] This may cause cell to return or not to a surface. Further, if interfacial forces are sufficient to alter the motor rotation, they may also be triggering cellular changes via the flagellar dynamometer mechanism[13] in ways that would not seem possible for non-swimmers that lack key motor

proteins. This possibility is particularly important because it implies that even without firm adhesion to a surface, bacterial virulence factors may be upregulated by dynamic surface contact. In this study, the mechanics of the nonadhesive surface produced difference in integrated bacteria-surface contact by a factor of three or more.

Conclusions

We demonstrated how *E. coli,* swimming in gentle shearing flow near hydrated PEG coatings, experience more extensive dynamic contact near stiffer hydrogel coatings and molecularly tethered PEG layers having lower water content than near softer more hydrated hydrogel coatings of otherwise identical chemistry. Greater dynamic contact was manifest in runs or "engagements" of longer durations for cell travel in the flow direction, and in a substantially greater tendency for swimming cells, traveling along the surface and then escaping, to return to the surface for engagements of additional dynamic contact. The tendency of swimming cells to escape and return to the stiffer less hydrated surfaces compared with the soft hydrogel was remarkable and clear, beyond several standard deviations of the return frequency. By contrast, near the softer hydrogels, swimming cells behaved similarly to a non-motile control. Similar behavior of swimmers near 100 μm-thick hydrogels and molecularly tethered layers suggests that only the outer few nanometers of the stiff coatings influence cell travel. The net effect of longer individual swimming engagements and a tendency for cells to return to the coating was that individual cells spent about three times the dynamic contact time on these coatings compared with softer more hydrated hydrogel coatings. While differences in the lubricity and wall slip of the coating, along with direct mechanical influence, may contribute to slight differences in the cell velocity, the dramatic differences in swimming character and return trajectories require an

explanation involving swimming itself: Either interaction with the coating directly influence flagellar rebundling or, forces from the flagellae on the motor influence its rotation and the frequency at which flagella unbundle and rebundle. To the extent that different surfaces influence flagellar bundling and rotation, there is the potential of the different surfaces to trigger, to different extents, virulence mechanisms that are initiated with flagellar restrictions.

Materials and Methods

Fabrication and Characterization of PEG Hydrogel Coatings. Previously established protocols[31, 52, 53] were employed in the preparation of "Soft" and "Stiff" PEG hydrogels. Solutions were formulated with 11 wt% and 55 wt% polyethylene glycol dimethacrylate (M_n 750 g/mol, Sigma-Aldrich, St. Louis, MO), respectively, which were dissolved in phosphate buffered saline that was sterile-filtered and degassed with nitrogen. The radical photo initiator, Irgacure 2959 (0.8 wt%, BASF Ludwigshafen, Germany) was added to the polymer precursor solution to facilitate photopolymerization. The hydrogel precursor solution was pipetted onto glass coverslips (Fisher Scientific, Fair Lawn, NJ) that were functionalized with 3-(trimethoxysilyl)propyl methacrylate (Sigma-Aldrich) to covalently attach the hydrogel to the coverslip. A 24 mm × 40 mm glass coverslip (Fisher Scientific) was placed on top of the hydrogel precursor solution to inhibit oxygen diffusion and to produce a uniform coating. Hydrogels were cured under UV light at 365 nm for 10 minutes. Following polymerization, the top coverslip was removed with forceps and the glass-bound hydrogels were equilibrated overnight in phosphate buffered saline. The hydrogel's were then trimmed, enabling a fit against the gasket of the flow chamber. The hydrogel coating thicknesses were determined using a digital micrometer (Mitutoyo Corporation, Kawaski, Japan) by averaging 5 measurements on each of at least 3 fully swollen hydrogels.

The hydrogel characterization in Table I was taken from a previous reference,[32] however, for clarity the characterization is summarized here. After equilibration in phosphate buffered saline, the swelling mass, M_S, and dried mass after lyophilization, M_D were measured. The equilibrated polymer concentration is the inverse of Q, which was defined as M_S / M_D was 8.6 ± 1.0 and 2.2 ±

0.05 for the soft and stiff hydrogels, respectively.[32] A modified Flory theory[54] was applied to determine the mesh size, ξ, from equation (1):

$$\xi = v_{2,s}^{-1/3}(\bar{r}^2)^{1/2} \quad (1)$$

where $v_{2,s}$ is the swollen volume fraction of the polymer and $(\bar{r}^2)^{1/2}$ is the average end-to-end distance of the crosslinked PEG.

Small amplitude oscillatory shear in a plate-plate geometry (Kinexus Pro Rheometer, Malvern Instruments, UK) was employed to determine the moduli of free-standing specimens. Moduli were measured at a strain of 0.1%, determined, based on a strain amplitude sweep, to be within the linear viscoelastic regime. Oscillation frequency sweeps were conducted over an angular frequency domain, 1.0 and 100 rad/s at 23 ºC.

Fabrication and Characterization of End-Tethered PEG Layers Established methods[39, 40] were employed to produce end tethered layers of polyethylene glycol (PEG) from the physisorption of Poly-L-lyine – PEG comb polymers onto acid etched glass. The cationic PLL backbones adsorb to the negatively charged silica, effectively tethering the PEG side chains. The resulting end-tethered layer of PEG chains have been proven, in many previous studies in our lab[33, 35, 39, 55-57] and the labs of others[6, 40, 41], to be exceptionally stable over the conditions and times scales of experiments, including exposure to varied ionic strength, pH, polymer solutions, particles, bacteria, and mammalian cells. In the current studies, no bacterial cells adhered to the coatings, an indication of both the robustness and stability of the PEG layers.

The synthesis of PLL-PEG copolymers followed the method of Kenausius *et al*. [39, 40, 57] Briefly, poly-L-lysine hydrobromide (PLL) with a nominal molecular weight of 20,000 g/mol (Sigma-

Aldrich, St. Louis) was dissolved in 50 mM sodium borate buffer (pH 9.1) and reacted with sufficient 5K molecular weight PEG sodium valeric acid (Laysan Bio Inc., Arab, AL) to functionalize the PLL by approximately one third. After purification by dialysis, freeze samples were stored at -20°C. Copolymers in D_2O were characterized using ^1H NMR on a Bruker 400 MHz instrument. The extent of PLL functionalization was determined from the relative areas of the lysine side chain peak (-CH_2-N-) at 2.909 ppm and the PEG peak (-CH_2-CH_2-) at 3.615 ppm.

FisherFinest microscope slides were prepared by soaking overnight in concentrated sulfuric acid, rinsing thoroughly in DI water, and immediately sealing them in a laminar flow chamber. After flowing 0.01 M phosphate buffer (0.008 M Na_2HPO_4 and 0.002 M KH_2PO_4), a 100 ppm copolymer solution in 0.01 M phosphate buffer was flowed over the surface for 20 minutes at a wall shear rate of 5.0 s^{-1} and then buffer was flowed again. Near-Brewster reflectometry[58] was employed as needed to monitor copolymer adsorption and to determine the adsorbed amount, near 1.1 mg/m^2, in order to enable calculations of the properties of the layers, in Table I.

<u>*Bacteria*</u>. *E. coli* JW1881 and *E. coli* JW1879 were purchased from the Coli Genetic Stock Center (New Haven, CT). These strains contain genetic knockouts of the flhD, which is critical for the growth of flagella[59] and of the motA gene, which is necessary for proton-conducting in the flagella motor, yet does not affect flagella synthesis,[60] respectively. In order to upregulate the growth of flagella, a pflhDC plasmid was cloned into both isogenic mutant strains. (Details of the design of this plasmid can be found in the Supporting Information.) Briefly, *E. coli* JW1881 or JW1879 was grown in Luria broth (LB Media) to an OD of 0.5, washed twice with ice cold deionized water and transformed with 100 ng of plasmid DNA using electroporation. (#FB101,

Fisher Scientific). Bacteria were recovered in LB Media for 30 minutes and plated on carbenicillin plates (Chem Impex international) overnight for subsequent studies. This produced a swimming strain and a non-motile strain both containing flagella.

Bacteria were grown in overnight at 37°C in LB Media with 50μg/mL kanamycin and 100μg/mL carbenicillin. After overnight growth liquid cultures were restarted using 200μL of overnight culture in mL of LB Media and the same antibiotics. Additionally, in the restarted cultures 50 μL of 20% wt/vol arabinose solution was added to induce the pflhDC plasmid. These cultures were grown for 4 hours and harvested in the log growth phase. Bacteria cultures were then washed 3 times (centrifuged at 3500 rpm for 2 min) in pH 7.4 Phosphate Buffered Saline (PBS) (0.008 M Na_2HPO_4, 0.002 M KH_2PO_4, and 0.15 M NaCl) and resuspended in the same buffer at a concentration of approximately $1x10^8$ cells/mL, based on OD600 measurements. This concentration is below that were bacteria-bacteria interactions were found relevant at surfaces.[61]

Bacteria Characterization. After the final growth step described above, bacteria were washed in deionized (DI) water 3 times and then fixed in 2.5% Glyceraldehyde solution in DI water for 2 hours followed 3 additional washes in DI water. 20 μL of resuspended bacteria solution was pipetted onto the center of a piece of a clean silicon wafer and allowed to air dry overnight. Samples were sputter coated (Cressington Sputter Coater 108) with gold for 60 seconds prior to imaging with a FEI Magellan 400 XHR-SEM.

The bulk solution swimming character of the of the motile *E. coli* was assessed in at a concentration of 9×10^7 cells/ml in phosphate buffered saline, employing a vertically oriented

chamber into which the suspension was injected using a syringe pump. Then with the pump turned off to achieve quiescent conditions, a lateral microscope fitted with a 20x objective was focused roughly 250 μm from the chamber wall, near the middle of the chamber. Video microsophy was recorded at 30 frames/seconds and subsequent particle tracking employed a self-written Python code. A 5 pixel (1.85 μm) maximum displacement for cell travel between frames was chosen for the linking rule. Trajectories lasting less than 5 seconds (due to cells exitting the focal plane) were discarded and the average time for the collected trajectories is 11.85 seconds.

Bacteria in Flow. The interactions between flowing bacteria and PEG coatings were studied using a custom-built flow chamber of dimensions 0.8 mm x 8 mm x 50 mm. The coated test surface of a microscope slide comprised one wall of the flow chamber, which was oriented vertically on an optical bench, with horizontal flow past that surface. This configuration eliminated gravitational forces normal to the surface. Videomicroscopy employed a Nikon Plan Fluor 20x objective with a numerical aperture of 0.5, producing a depth of field of approximately 3.5μm. Bacteria were flowed across the surface at a shear rate of 15 s^{-1} for approximately 10 minutes. Data were recorded on DVDs and analyzed at a rate of 5 frames per second using FFmpeg software. Manual tracking employed FIJI is just ImageJ. In the analysis, all cells meeting the criteria for engagement, that were visible in the run, were analyzed. We found that, in a given run, the behavior of cells in the early minutes of the run was statistically identical to that of the cells towards the end of the run.

Acknowledgements. Sincere thanks go to S. Riverez and the Siegrist lab at the University of Massachusetts at Amherst for providing support by growing bacteria for swimming

characterization studies. Additionally we are grateful to K. Kolewe of the Schiffman Lab at the University of Massachusetts for growing some bacteria, providing some hydrogel films and teaching MKS the methodology for growing and handling bacteria and casting thin hydrogel films. We are also grateful to the Schiffman and Siegrist labs for use of their facilities for growing bacteria. The work was made possible by funding from the National Science Foundation CBET 1848065 and NIH traineeships to M. K. Shave under NIH National Research Service Award GM008515.

References

1. Donlan, R. M.; Costerton, J. W. Biofilms: Survival mechanisms of clinically relevant microorganisms. *Clinical Microbiology Reviews* **2002**, *15*, 167-193.

2. Banerjee, I.; Pangule, R. C.; Kane, R. S. Antifouling Coatings: Recent Developments in the Design of Surfaces That Prevent Fouling by Proteins, Bacteria, and Marine Organisms. *Adv. Mater.* **2011**, *23*, 690-718.

3. Ekblad, T.; Bergstroem, G.; Ederth, T.; Conlan, S. L.; Mutton, R.; Clare, A. S.; Wang, S.; Liu, Y. L.; Zhao, Q.; D'Souza, F.; Donnelly, G. T.; Willemsen, P. R.; Pettitt, M. E.; Callow, M. E.; Callow, J. A.; Liedberg, B. Poly(ethylene glycol)-Containing Hydrogel Surfaces for Antifouling Applications in Marine and Freshwater Environments. *Biomacromolecules* **2008**, *9*, 2775-2783.

4. Otsuka, H.; Nagasaki, Y.; Kataoka, K. PEGylated nanoparticles for biological and pharmaceutical applications. *Adv. Drug Deliv. Rev.* **2003**, *55*, 403-419.

5. Carnt, N. A.; Evans, V. E.; Naduvilath, T. J.; Willcox, M. D. P.; Papas, E. B.; Frick, K. D.; Holden, B. A. Contact Lens-Related Adverse Events and the Silicone Hydrogel Lenses and Daily Wear Care System Used. *Archives of Ophthalmology* **2009**, *127*, 1616-1623.

6. Harris, L. G.; Tosatti, S.; Wieland, M.; Textor, M.; Richards, R. G. Staphylococcus aureus adhesion to titanium oxide surfaces coated with non-functionalized and peptide-functionalized poly(L-lysine)-grafted-poly(ethylene glycol) copolymers. *Biomaterials* **2004**, *25*, 4135-4148.

7. Wang, Y.; Guan, A.; Isayeva, I.; Vorvolakos, K.; Das, S.; Li, Z. Y.; Phillips, K. S. Interactions of Staphylococcus aureus with ultrasoft hydrogel biomaterials. *Biomaterials* **2016**, *95*, 74-85.

8. Willcox, M. D. P.; Harmis, N.; Cowell, B. A.; Williams, T.; Holden, B. A. Bacterial interactions with contact lenses; effects of lens material, lens wear and microbial physiology. *Biomaterials* **2001**, *22*, 3235-3247.

9. Funt, D.; Pavicic, T. Dermal Fillers in Aesthetics: An Overview of Adverse Events and Treatment Approaches. *Clin. Cosmet. Investig. Dermatol.* **2013**, *6*, 295-316.

10. Park, K. D.; Kim, Y. S.; Han, D. K.; Kim, Y. H.; Lee, E. H. B.; Suh, H.; Choi, K. S. Bacterial adhesion on PEG modified polyurethane surfaces. *Biomaterials* **1998**, *19*, 851-859.

11. Costerton, J. W.; Lappin-Scott, H. M., Introduction to microbialbiofilms. In *Microbial biofilms*, Costerton, J. W., Ed. Cambridge University Press: Cambridge, United Kingdom, 1995; pp 1-11.

12. Davies, D. G.; Geesey, G. G. Regulation of the Alginate Biosynthesis Gene ALGC in Pseudomonas aeruginosa during Biofilm Development in Continuous Culture *Applied and Environmental Microbiology* **1995**, *61*, 860-867.

13. McCarter, L.; Hilmen, M.; Silverman, M. Flagellar Dynomometer Controls Swarmer Cell-Differentiation of V-Parahaemolyticus. *Cell* **1988**, *54*, 345-351.

14. Persat, A.; Nadell, C. D.; Kim, M. K.; Ingremeau, F.; Siryaporn, A.; Drescher, K.; Wingreen, N. S.; Bassler, B. L.; Gitai, Z.; Stone, H. A. The Mechanical World of Bacteria. *Cell* **2015**, *161*, 988-997.

15. Frymier, P. D.; Ford, R. M.; Berg, H. C.; Cummings, P. T. 3-Dimensional Tracking of Motile Bacteria near a Solid Planar Surface *Proc. Natl. Acad. Sci. U. S. A.* **1995**, *92*, 6195-6199.

16. Vigeant, M. A. S.; Ford, R. M. Interactions between motile Escherichia coli and glass in media with various ionic strengths, as observed with a three-dimensional-tracking microscope. *Applied and Environmental Microbiology* **1997**, *63*, 3474-3479.

17. DiLuzio, W. R.; Turner, L.; Mayer, M.; Garstecki, P.; Weibel, D. B.; Berg, H. C.; Whitesides, G. M. Escherichia coli swim on the right-hand side. *Nature* **2005**, *435*, 1271-1274.

18. Vigeant, M. A. S.; Ford, R. M.; Wagner, M.; Tamm, L. K. Reversible and irreversible adhesion of motile Escherichia coli cells analyzed by total internal reflection aqueous fluorescence microscopy. *Applied and Environmental Microbiology* **2002**, *68*, 2794-2801.

19. Gent, A. N. Adhesion and strength of viscoelastic solids. Is there a relationship between adhesion and bulk properties? *Langmuir* **1996**, *12*, 4492-4496.

20. Berke, A. P.; Turner, L.; Berg, H. C.; Lauga, E. Hydrodynamic attraction of swimming microorganisms by surfaces. *Phys. Rev. Lett.* **2008**, *101*.

21. Li, G. L.; Bensson, J.; Nisimova, L.; Munger, D.; Mahautmr, P.; Tang, J. X.; Maxey, M. R.; Brun, Y. V. Accumulation of swimming bacteria near a solid surface. *Phys. Rev. E* **2011**, *84*.

22. Lauga, E.; DiLuzio, W. R.; Whitesides, G. M.; Stone, H. A. Swimming in circles: Motion of bacteria near solid boundaries. *Biophys. J.* **2006**, *90*, 400-412.

23. Li, G. L.; Tang, J. X. Accumulation of Microswimmers near a Surface Mediated by Collision and Rotational Brownian Motion. *Phys. Rev. Lett.* **2009**, *103*.

24. Di Leonardo, R.; Dell'Arciprete, D.; Angelani, L.; Iebba, V. Swimming with an Image. *Phys. Rev. Lett.* **2011**, *106*.

25. Hu, J. L.; Wysocki, A.; Winkler, R. G.; Gompper, G. Physical Sensing of Surface Properties by Microswimmers - Directing Bacterial Motion via Wall Slip. *Sci Rep* **2015**, *5*.

26. Lemelle, L.; Palierne, J. F.; Chatre, E.; Place, C. Counterclockwise Circular Motion of Bacteria Swimming at the Air-Liquid Interface. *J. Bacteriol.* **2010**, *192*, 6307-6308.

27. Rusconi, R.; Guasto, J. S.; Stocker, R. Bacterial transport suppressed by fluid shear. *Nat. Phys.* **2014**, *10*, 212-217.

28. Kaya, T.; Koser, H. Direct Upstream Motility in Escherichia coli. *Biophys. J.* **2012**, *102*, 1514-1523.

29. Marcos; Fu, H. C.; Powers, T. R.; Stocker, R. Bacterial rheotaxis. *Proc. Natl. Acad. Sci. U. S. A.* **2012**, *109*, 4780-4785.

30. Qu, Z. J.; Temel, F. Z.; Henderikx, R.; Breuer, K. S. Changes in the flagellar bundling time account for variations in swimming behavior of flagellated bacteria in viscous media. *Proc. Natl. Acad. Sci. U. S. A.* **2018**, *115*, 1707-1712.

31. Kolewe, K. W.; Peyton, S. R.; Schiffman, J. D. Fewer Bacteria Adhere to Softer Hydrogels. *ACS Appl. Mater. Interfaces* **2015**, *7*, 19562-19569.

32. Kolewe, K. W.; Kalasin, S.; Shave, M.; Schiffman, J. D.; Santore, M. M. Mechanical Properties and Concentrations of Poly(ethylene glycol) in Hydrogels and Brushes Direct the Surface Transport of Staphylococcus aureus. *ACS Appl. Mater. Interfaces* **2019**, *11*, 320-330.

33. Gon, S.; Fang, B.; Santore, M. M. Interaction of Cationic Proteins and Polypeptides with Biocompatible Cationically-Anchored PEG Brushes. *Macromolecules* **2011**, *44*, 8161-8168.

34. Bloustine, J.; Virmani, T.; Thurston, G. M.; Fraden, S. Light scattering and phase behavior of lysozyme-poly(ethylene glycol) mixtures. *Phys. Rev. Lett.* **2006**, *96*, 087803.

35. Kalasin, S.; Santore, M. M. Near-Surface Motion and Dynamic Adhesion during Silica Microparticle Capture on a Polymer (Solvated PEG) Brush via Hydrogen Bonding. *Macromolecules* **2016**, *49*, 334-343.

36. Ishida, T.; Wang, X.; Shimizu, T.; Nawata, K.; Kiwada, H. PEGylated liposomes elicit an anti-PEG IgM response in a T cell-independent manner. *J. Control. Release* **2007**, *122*, 349-355.

37. Liu, Y. J.; Reidler, H.; Pan, J.; Milunic, D.; Qin, D. J.; Chen, D.; Vallejo, Y. R.; Yin, R. A double antigen bridging immunogenicity ELISA for the detection of antibodies to polyethylene glycol polymers. *J. Pharmacol. Toxicol. Methods* **2011**, *64*, 238-245.

38. Canal, T.; Peppas, N. A. Correlation between Mesh Size and Equilibrium Degree of Swelling of Polymeric Networks *J. Biomed. Mater. Res.* **1989**, *23*, 1183-1193.

39. Gon, S.; Bendersky, M.; Ross, J. L.; Santore, M. M. Manipulating Protein Adsorption using a Patchy Protein-Resistant Brush. *Langmuir* **2010**, *26*, 12147-12154.

40. Kenausis, G. L.; Voros, J.; Elbert, D. L.; Huang, N. P.; Hofer, R.; Ruiz-Taylor, L.; Textor, M.; Hubbell, J. A.; Spencer, N. D. Poly(L-lysine)-g-poly(ethylene glycol) layers on metal oxide surfaces: Attachment mechanism and effects of polymer architecture on resistance to protein adsorption. *J. Phys. Chem. B* **2000**, *104*, 3298-3309.

41. Dalsin, J. L.; Lin, L. J.; Tosatti, S.; Voros, J.; Textor, M.; Messersmith, P. B. Protein resistance of titanium oxide surfaces modified by biologically inspired mPEG-DOPA. *Langmuir* **2005**, *21*, 640-646.

42. Alexander, S. Adsorption of Chain Molecules with a Polar Head A Acaling Description. *Journal De Physique* **1977**, *38*, 983-987.

43. Milner, S. T. Polymer Brushes. *Science* **1991**, *251*, 905-914.

44. Gon, S.; Kumar, K. N.; Nusslein, K.; Santore, M. M. How Bacteria Adhere to Brushy PEG Surfaces: Clinging to Flaws and Compressing the Brush. *Macromolecules* **2012**, *45*, 8373-8381.

45. Grest, G. S., Normal and shear forces between polymer brushes. In *Polymers in Confined Environments*, Granick, S., Ed. 1999; Vol. 138, pp 149-183.

46. Lai, P. Y.; Binder, K. Grafted Polymer Layers Under Shear - A Monte-Carlo Simulation *J. Chem. Phys.* **1993**, *98*, 2366-2375.

47. Milner, S. T. Hydrodynamic Penetration into Parabolic Brushes. *Macromolecules* **1991**, *24*, 3704-3705.

48. Goldman, A. J.; Cox, R. G.; Brenner, H. Slow Viscous Motion of a Sphere Parallel to a Plane Wall. 2. Couette Flow. *Chem. Eng. Sci.* **1967**, *22*, 653-660.

49. McClaine, J. W.; Ford, R. M. Reversal of flagellar rotation is important in initial attachment of Escherichia coli to glass in a dynamic system with high- and low-ionic-strength buffers. *Applied and Environmental Microbiology* **2002**, *68*, 1280-1289.

50. Patteson, A. E.; Gopinath, A.; Goulian, M.; Arratia, P. E. Running and tumbling with E-coli in polymeric solutions. *Sci Rep* **2015**, *5*.

51. Chattopadhyay, S.; Moldovan, R.; Yeung, C.; Wu, X. L. Swimming efficiency of bacterium Escherichia coli. *Proc. Natl. Acad. Sci. U. S. A.* **2006**, *103*, 13712-13717.

52. Peyton, S. R.; Raub, C. B.; Keschrumrus, V. P.; Putnam, A. J. The use of poly(ethylene glycol) hydrogels to investigate the impact of ECM chemistry and mechanics on smooth muscle cells. *Biomaterials* **2006**, *27*, 4881-4893.

53. Herrick, W. G.; Nguyen, T. V.; Sleiman, M.; McRae, S.; Emrick, T. S.; Peyton, S. R. PEG-Phosphorylcholine Hydrogels As Tunable and Versatile Platforms for Mechanobiology. *Biomacromolecules* **2013**, *14*, 2294-2304.

54. Canal, T.; Peppas, N. A. Correlation between Mesh Size and Equiibrium Degree of Swelling of Polymeric Networks. *Journal of Biomedical Materials Research* **1989**, *23*, 1183-1193.

55. Fang, B.; Gon, S.; Nusslein, K.; Santore, M. M. Surfaces for Competitive Selective Bacterial Capture from Protein Solutions. *ACS Appl. Mater. Interfaces* **2015**, *7*, 10275-10282.

56. Kalasin, S.; Browne, E. P.; Arcaro, K. F.; Santore, M. M. Surfaces that Adhesively Discriminate Breast Epithelial Cell Lines and Lymphocytes in Buffer and Human Breast Milk. *ACS Appl. Mater. Interfaces* **2019**, *11*, 16347-16356.

57. Huang, N. P.; Michel, R.; Voros, J.; Textor, M.; Hofer, R.; Rossi, A.; Elbert, D. L.; Hubbell, J. A.; Spencer, N. D. Poly(L-lysine)-g-poly(ethylene glycol) layers on metal oxide surfaces: Surface-analytical characterization and resistance to serum and fibrinogen adsorption. *Langmuir* **2001**, *17*, 489-498.

58. Fu, Z. G.; Santore, M. M. Poly(ethylene oxide) adsorption onto chemically etched silicates by Brewster angle reflectivity. *Colloid Surface A* **1998**, *135*, 63-75.

59. Liu, X. Y.; Matsumura, P. The FLHD FLHC Complex, A Transcriptional Activator of the Eschericia-Coli Flagellar Class-II Operons. *J. Bacteriol.* **1994**, *176*, 7345-7351.

60. Nguyen, C. C.; Saier, M. H. Structural and phylogenetic analysis of the MotA and MotB families of bacterial flagellar motor proteins. *Res. Microbiol.* **1996**, *147*, 317-332.

61. Fang, B.; Gon, S.; Park, M.; Kumar, K. N.; Rotello, V. M.; Nusslein, K.; Santore, M. M. Bacterial adhesion on hybrid cationic nanoparticle-polymer brush surfaces: Ionic strength tunes capture from monovalent to multivalent binding. *Colloid Surf. B-Biointerfaces* **2011**, *87*, 109-115.